Neuron, Volume 64

Supplemental Data

Neural "Ignition": Enhanced Activation Linked to Perceptual Awareness in Human Ventral Stream Visual Cortex

Lior Fisch, Eran Privman, Michal Ramot, Michal Harel, Yuval Nir, Svetlana Kipervasser, Fani Andelman, Miri Y. Neufeld, Uri Kramer, Itzhak Fried, and Rafael Malach

Table S1: Recording Details

Subject	Gender	Electrode type	Talairach coordinates		
P12	F	H	L58	P58	I11
		H	L52	P69	I8
		H	L51	P67	I14
		H	L47	P79	I15
		L	L37	P84	I20
		L	L27	P88	I25
		L	L13	P93	I29
		H	n/a	n/a	n/a
P13	F	O	L49	P9	S31
		O	L48	P17	S38
P15	F	L	L25	P87	S2
		L	L18	P94	I4
		L	L15	P94	I9
		L	L12	P94	I14
P17	F	H	L50	P58	I18
		H	L41	P56	I20
		H	L30	P54	I18
		L	R7	P83	I18
		L	R17	P78	I18
		L	R27	P74	I18
		H	R36	P69	I18
		H	R44	P65	I16
		H	R51	P61	I10
P19	F	H	L38	P45	I27
P20	M	H	L42	P75	S3
		H	L40	P40	I23
		H	L33	P83	S5
		H	L31	P42	I21
P21	M	L	R17	P95	I4
		H	R39	P87	I18
		H	R42	P81	I11
P22	M	H	L52	P53	I23
		H	L42	P56	I23
		H	L32	P60	I20
P23	F	H	L38	P82	S14
		L	R32	P66	I14

		H	R36	P80	S11
		H	R41	P68	I15
P24	M	H	L52	P60	I15
		H	L40	P56	I15
		H	L32	P49	I15
		H	L24	P43	I16
		H	R36	P29	I26
		O	R40	P7	I33
		H	R43	P34	I26
		H	R51	P42	I26
		H	R58	P47	I19
		H	R62	P47	I12

Table S1. Details of all task-related electrodes. Electrode type: L = low-level visual cortex, H = high-level visual cortex, O = other (non-visual cortex).

Table S2: Target-selective electrodes

Subject	Talairach coordinates			Preferred category	Gamma BLP effect	*p* value	Evoked effect	N170 effect
P12	L51	P67	I14	F	yes	3.46E-03	yes	no
	L58	P58	I11	F	yes	9.26E-04	yes	no
	L47	P79	I15	F	yes	9.33E-03	yes	no
	L52	P69	I8	F	yes	1.53E-03	yes	no
P17	L41	P56	I20	T	yes	1.24E-03	no	-
	L50	P58	I18	F	no	3.31E-01	no	-
	R36	P69	I18	F	yes	1.11E-03	yes	yes
	R44	P65	I16	F	yes	6.51E-06	yes	yes
P19	L38	P45	I27	F	yes	2.74E-06	yes	yes
P20	L31	P42	I21	T	yes	9.92E-07	yes	no
	L40	P40	I23	F	yes	1.94E-03	no	no
	L42	P75	S3	F	no	1.50E-02	yes	-
P21	R39	P87	I18	F	no	1.78E-01	yes	no
	R42	P81	I11	F	no	1.28E-01	yes	no
P22	L32	P60	I20	F	yes	1.40E-04	yes	yes
P24	L32	P49	I15	T	yes	1.09E-03	yes	no
	L40	P56	I15	T	yes	1.05E-04	yes	yes
	L52	P60	I15	T	yes	1.68E-04	no	no
	R36	P29	I26	F	yes	1.65E-05	yes	yes

Table S2. Details of target-selective electrode responses (effect of recognition). Preferred category: F = faces, T = man-made objects ("tools"). N170 effect not defined for electrodes without a N170 component.

Table S3: Behavioral data

Face stimuli

SOA (ms)	% hits	% misses	% false alarm 1 ("house")	% false alarm 2 ("object")
16	54.0 ± 9.9	39.6 ± 11.2	5.7 ± 2.9	0.7 ± 0.3
33	63.1 ± 9.2	35.9 ± 9.5	0.7 ± 0.7	0.3 ± 0.3
50	85.3 ± 7.8	14.7 ± 7.8	-	-
66	90.9 ± 4.2	7.5 ± 4.7	1.5 ± 1.1	-
83	-	-	-	-
100	90.0	10.0	-	-
150	99.4	0.6	-	-
200	97.1 ± 1.5	2.6 ± 1.4	0.3 ± 0.2	-

House stimuli

SOA (ms)	% hits	% misses	% false alarm 1 ("face")	% false alarm 2 ("object")
16	37.1 ± 10.8	56.2 ± 12.9	1.8 ± 1.5	4.8 ± 2.1
33	26.8 ± 6.8	65.8 ± 9.2	2.4 ± 1.2	5.0 ± 2.5
50	53.6 ± 10.3	41.6 ± 11.6	0.5 ± 0.5	4.3 ± 2.5
66	45.1 ± 14.1	51.3 ± 14.2	1.3 ± 1.3	2.4 ± 1.8
83	82.5	17.5	-	-
100	80.0	10.0	10.0	-
150	89.3	7.1	-	3.6
200	99.1 ± 0.4	0.1 ± 0.1	0.2 ± 0.2	0.5 ± 0.4

Object stimuli

SOA (ms)	% hits	% misses	% false alarm 1 ("face")	% false alarm 2 ("house")
16	10.7 ± 2.9	63.3 ± 13.2	4.3 ± 1.8	21.7 ± 10.5
33	23.6 ± 7.0	63.7 ± 9.1	6.4 ± 2.5	6.3 ± 3.2
50	46.5 ± 7.4	48.2 ± 7.1	3.0 ± 1.4	2.3 ± 1.6
66	25.5 ± 12.2	68.8 ± 12.9	1.3 ± 1.3	4.4 ± 3.1
83	80.25	18.52	-	1.23
100	-	-	-	-
150	97.37	-	2.63	-
200	96.5 ± 1.2	2.8 ± 1.2	0.0 ± 0.0	0.7 ± 0.4

Table S3. Behavioral details, BM experiment. For each target category and SOA, rates (mean ± s.e.m. across relevant subjects) are given for all 4 possible trial outcomes: hits (correct recognition), misses (failure to recognize) and 2 types of false alarms (naming one of the two non-target categories). See also Figure S12.

Supplemental Figures

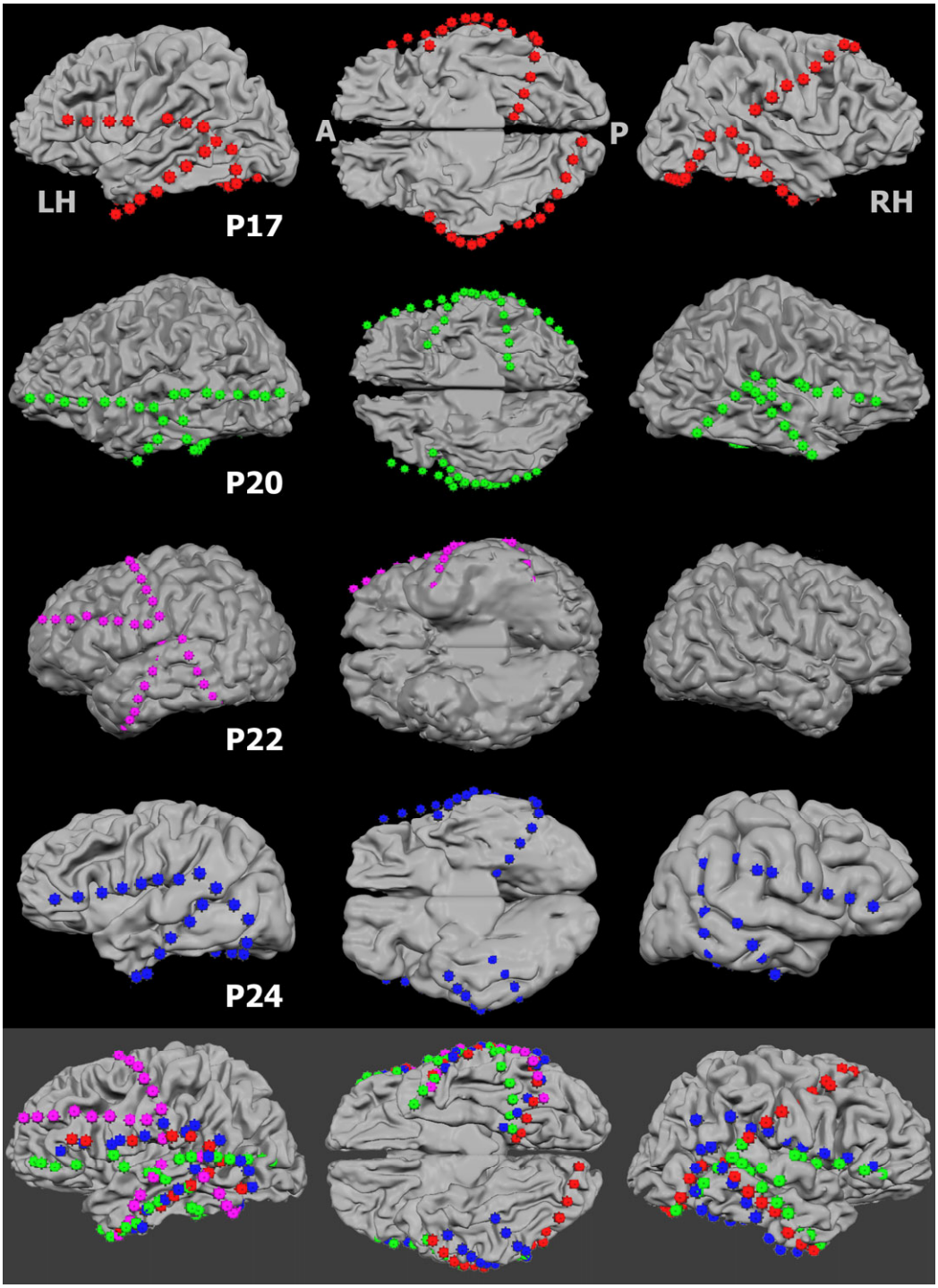

Figure S1. Electrode placements on individually reconstructed brains. Examples of reconstructions of cortical surfaces in 4 patients. Cortical surfaces were obtained for each patient using structural MRI scans, and electrode locations were derived from CT scans. The two data sets were then precisely

aligned and fused (see Experimental Procedures). Each row depicts data from a single patient (numbered). The left and right panels depict left and right hemispheres respectively shown from a side view, while the central panels depict the two hemispheres from a ventral view. The electrode sets from each patient are color-coded and positioned on the summary figure (bottom row). The cortical surface and electrode placements of the summary figure are the same as in Figure 1 (but without projection on the curved surface). Note that the data from all 11 patients in the study were processed in a similar manner, allowing the precise anatomical delineation of every electrode location.

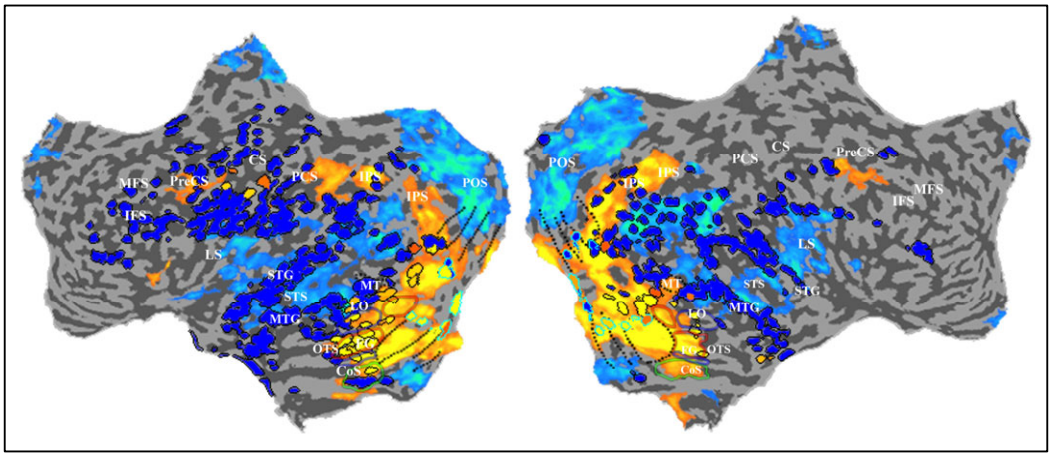

Figure S2. Location of the entire electrode set relative to visually activated and inactivated regions. The electrode locations are depicted superimposed on cortical regions activated (yellow) and inactivated (blue) during 1-back memory task while viewing static images of faces, houses, objects and patterns during fMRI mapping (Levy et al., 2001).

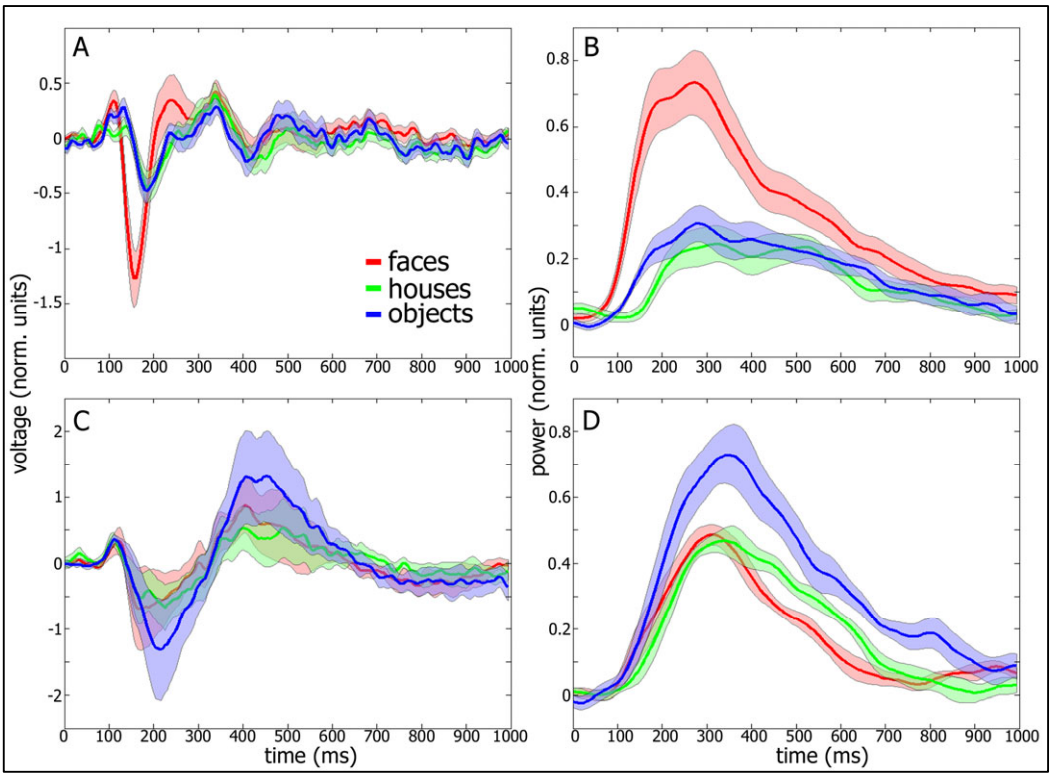

Figure S3. Selectivity in the backward masking task, target-selective visual electrodes. Mean responses to specific image categories are shown. Target duration = 16 ms, SOA = 200 ms. (A) Mean evoked response in electrodes responding preferentially to the face category (N = 14 electrodes). (B) Mean gamma power changes in response to these stimuli. (C-D) Same as (A-B), but for electrodes responding preferentially to the man-made objects category (N = 5 electrodes).

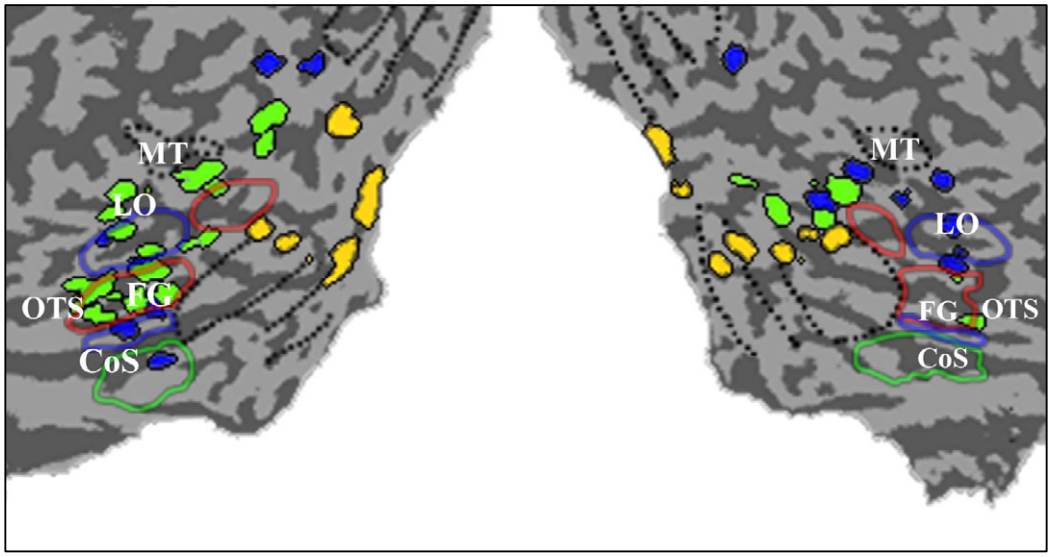

Figure S4. Responsive low-order (orange), high-order target-selective (green) and non-selective (blue) electrode locations. Retinotopic borders (dotted lines) and category-selective regions (colored contours, same convention as Figure 1) from independent fMRI experiments using a 1-back memory task of various image categories (similar to Figure S2). Enlarged view of occipital portion of the cortex is shown.

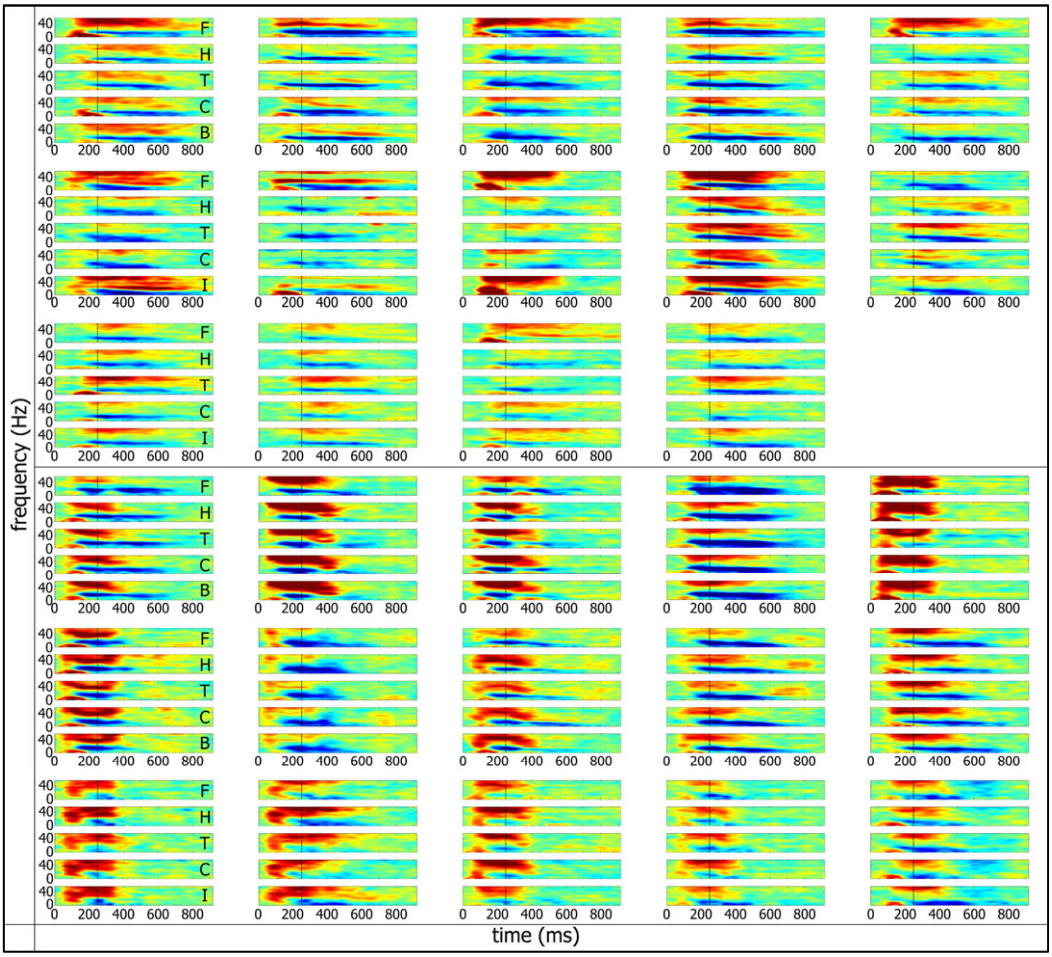

Figure S5. Time-frequency decomposition of short-mid latency visual electrode responses in the object categorization experiment. Figure depicts high order target-selective (upper panel) and low order (lower panel) electrodes. Each row depicts the response to one object category (F-faces, H-houses, T-man-made objects, C- cars, B/I- birds or inverted faces). Note the short latency and lack of selectivity characteristic of low order electrodes vs. the high object selectivity typical of high order electrodes.

Figure S6. Example of stimuli used in the backward masking experiment. Entire set of faces used with patients P21-P24 is shown, together with ratio of recognized trials to total number of trials with these images at the critical SOA (33ms for all 4 patients).

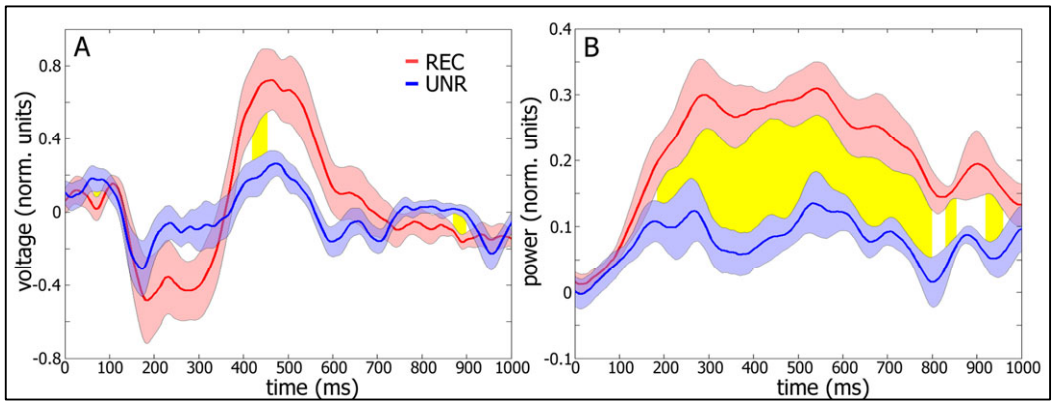

Figure S7. Average evoked and gamma power response of all object-selective electrodes. Same analysis as Figure 6A and 6C (see Experimental Procedures) but for (target-selective) man-made object-selective electrodes. (A) Grand average of evoked target responses in the backward masking experiment around the critical SOA (±16.66 ms) after subtracting the mask-only response. Means are shown for recognized (red) vs. unrecognized (blue) conditions; yellow region indicates time points in which the two responses differed significantly ($p < 0.01$, paired t test). The trial composition of both conditions is identical in terms of target stimulus identity, but not SOA. Error bars denote s.e.m. across electrodes (N=5 electrodes). (B) Same analysis as A, but for gamma BLP.

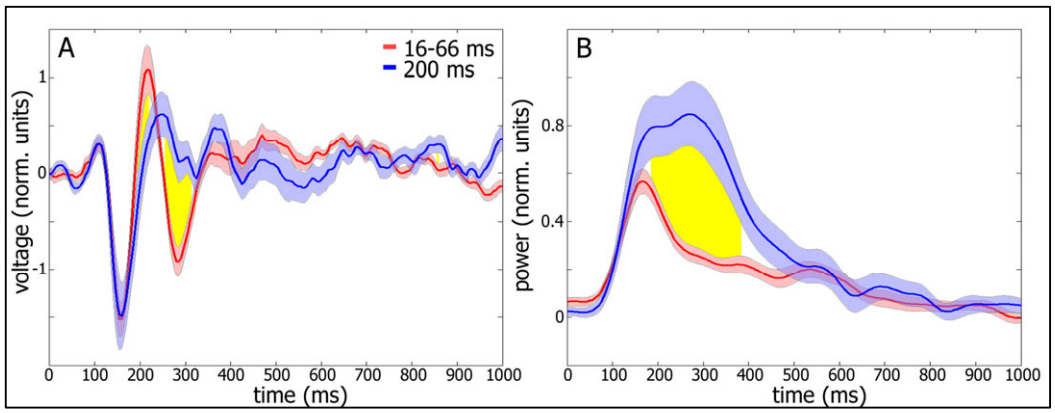

Figure S8. Average evoked and gamma power responses for short and long SOA. (A) Grand average of evoked target responses of all 14 face-selective electrodes to face targets in recognized trials at short (16-66 ms, red) and long (200 ms, blue) SOA. Data was collapsed across SOAs and then electrodes, after subtracting the mask-only response. Yellow region indicates time points in which the two responses differed significantly ($p < 0.01$, paired t test). (B) Same analysis as A, but for induced gamma power.

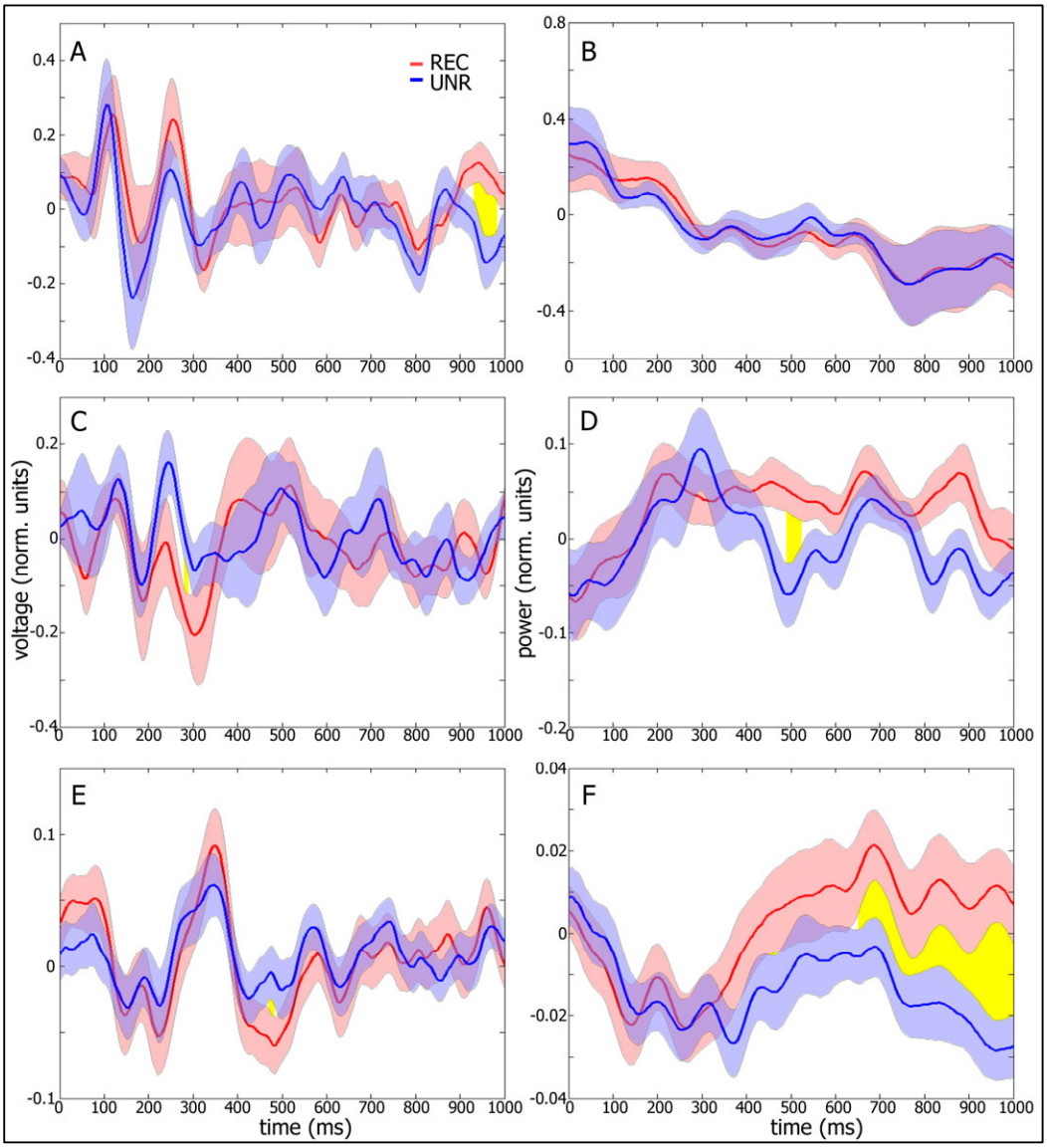

Figure S9. Average evoked and gamma power responses of all non target-selective electrodes. Same group analysis as in Figures 6 and S7 for 3 other responsive electrode categories. Responses shown are to all stimulus categories. The trial composition of both conditions is identical in terms of target stimulus identity, but not SOA (see Experimental Methods). (A) Grand average of evoked response from all responsive low-level electrodes (N=12 electrodes). (B) Average of gamma BLP response from same electrodes. (C-D) Responsive high-order, non target-selective electrodes (N=10). (E-F) Electrodes showing only evoked response within 250 ms of target stimulus onset, located outside of visual cortex (N=77).

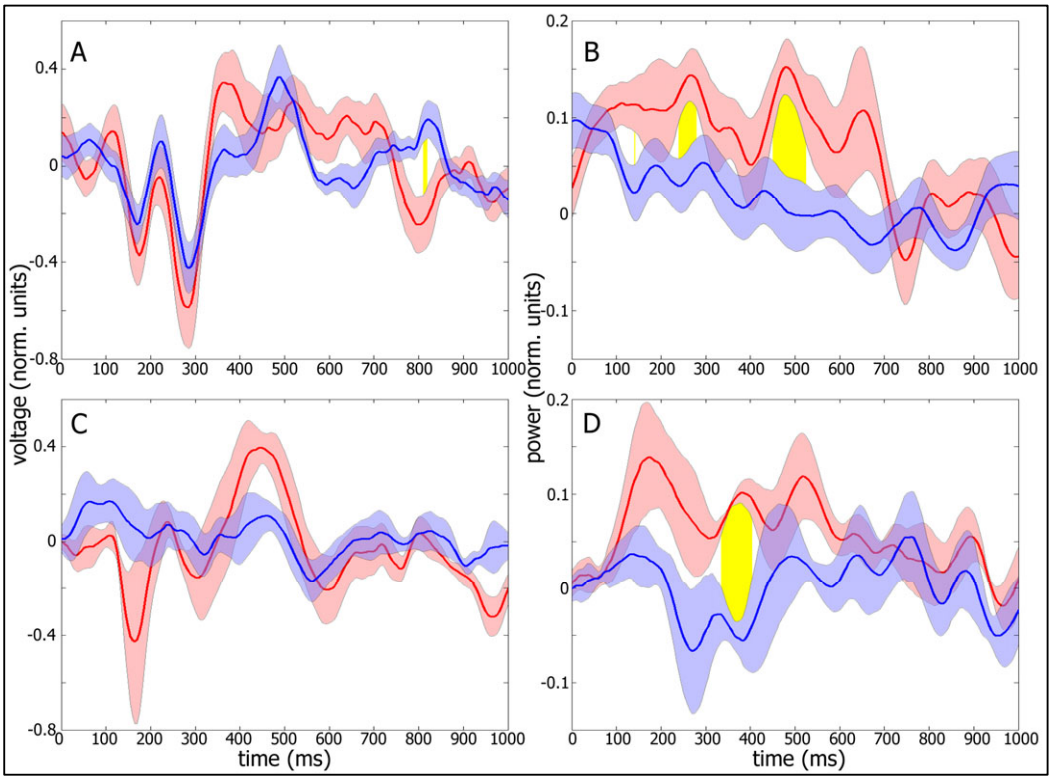

Figure S10. Average evoked and gamma power responses of all target-responsive electrodes to the non-preferred category. Grand average of target responses in the Backward Masking experiment around the critical SOA. Same group analysis as in Figures 6 and S7. (A) Evoked response and (B) Gamma BLP response of face electrodes (N=14) to man-made object category. (C) and (D) Same as (A) and (B) but for man-made object electrodes to face category.

Yellow regions denote points of significant difference in response between the two conditions ($p < 0.01$, paired t test).

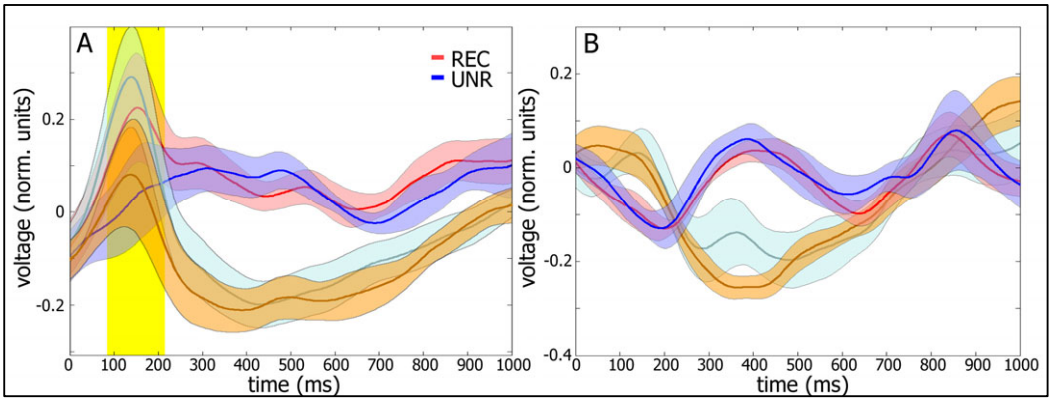

Figure S11. Average low-frequency power responses of target-responsive electrodes to the preferred category. Grand average of target responses in the BM experiment around the critical SOA. Same group analysis as in Figures 6 and S7 but for the low frequency bands of the LFP. (A) Mean low-frequency (15-25 Hz) BLP blank-subtracted response of face electrodes (N=14) in recognition (red) and no-recognition (blue) trials. Yellow regions denote points of significant difference in response between the two conditions ($p < 0.01$, paired t test). Orange (recognition) and cyan (no-recognition) plots show means before subtraction of blank response (not balanced for stimulus identity). Note that the difference in response occurs before the onset of ERD, and reflects the evoked N170 component. (B) Same analysis for man-made object electrodes (N=5).

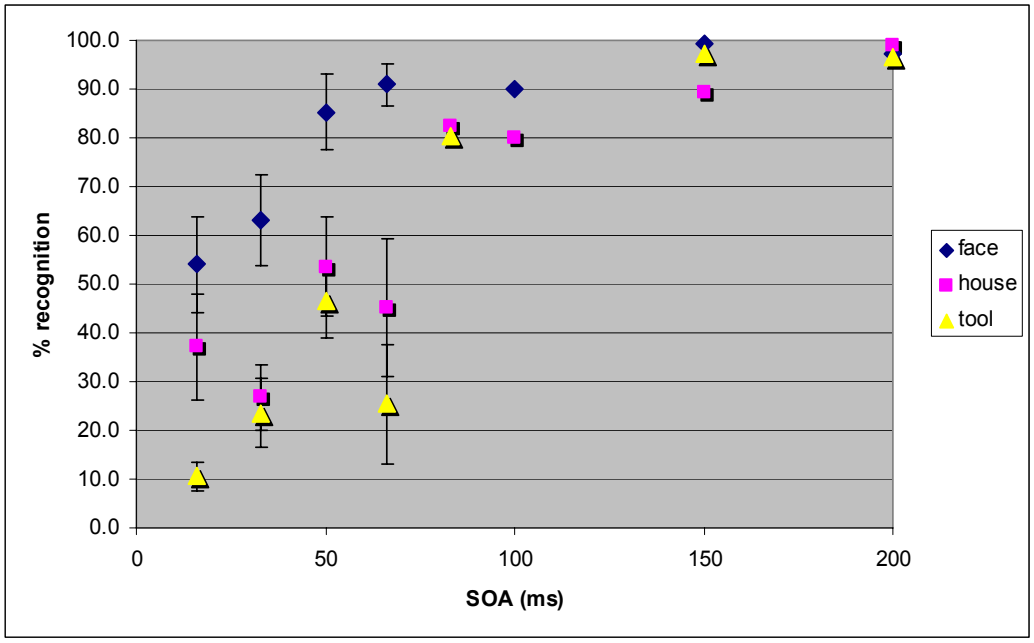

Figure S12. Behavioral data. Percentage of hits (successful recognition trials) out of all trials for a given category and SOA**.** Error bars denote s.e.m. across subjects**.**

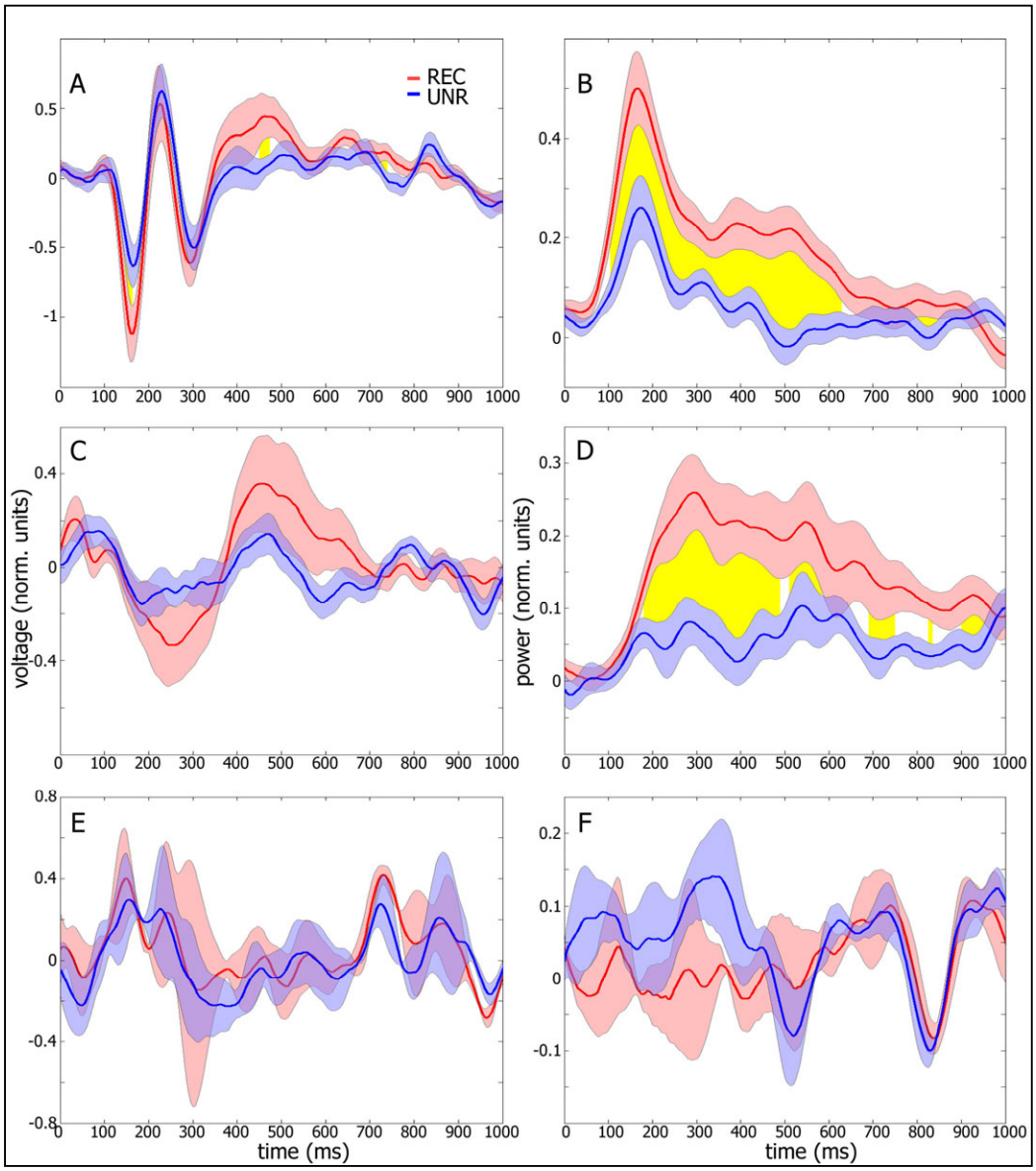

Figure S13. Grand averages in BM experiment of electrodes selected by OC experiment. Same comparison and averaging as in Figure 6 for electrodes grouped by selectivity in the OC experiment. Means are shown for recognition (red) vs. no-recognition (blue) conditions; yellow region indicates time points in which the two responses differed significantly ($p < 0.01$, paired t test). Shown are all electrodes in high-order visual cortex (as defined by BOLD maps, see text) which had a significantly larger gamma BLP response (t test, $p < 0.01$) in the OC experiment to one category (either faces, houses or man-made objects) than to the other two (see Experimental Procedures). (A) Evoked and (B) Gamma BLP response of face-selective electrodes (N=15). (C) Evoked and (D) Gamma BLP response of object-selective electrodes (N=7). (E) Evoked and (F) Gamma BLP response of house-selective electrodes (N=3).

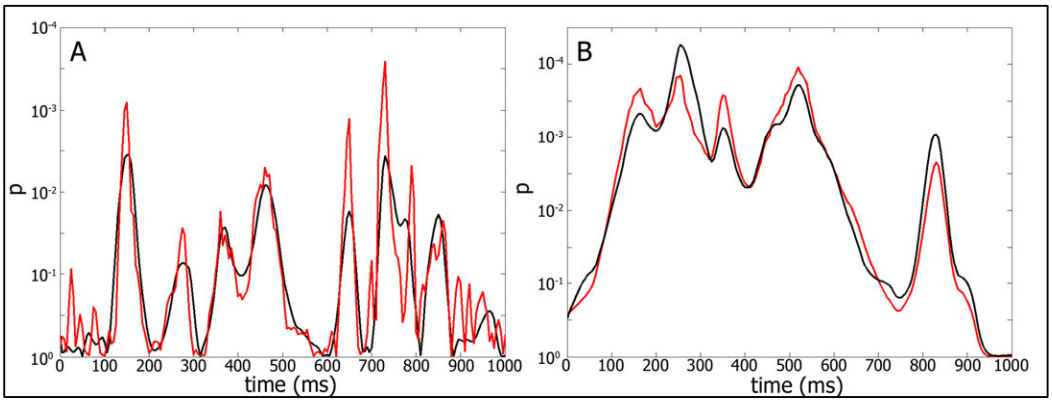

Figure S14. Shuffle control for Figure 6. Significance of difference in response, per time point, between recognition and no-recognition conditions in grand averages of target-selective face electrodes (N=14). Red line shows *p* values obtained from shuffle control (10^5 iterations, see Experimental Procedures) and black line shows conventional paired *t* test *p* values (see Figure 6 for details), in logarithmic scale, for (A) Evoked response difference (2-tailed), (B) Gamma BLP response difference (1-tailed, i.e. recognition > no-recognition).

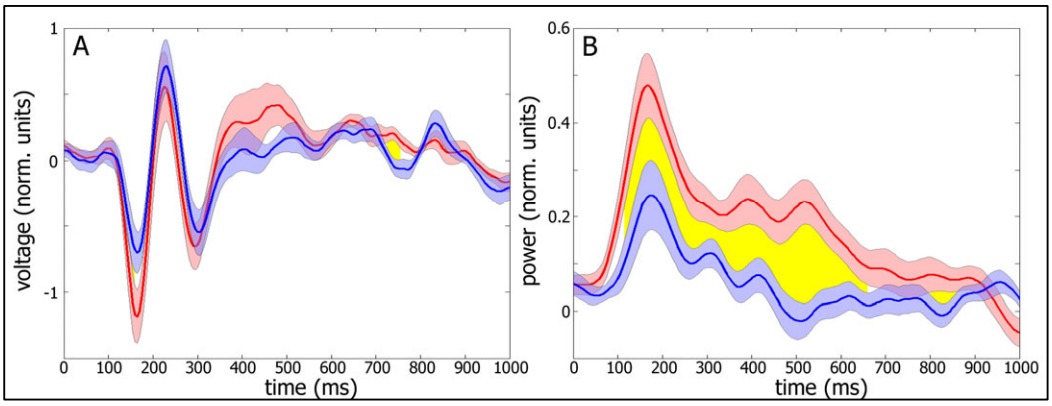

Figure S15. Average evoked and gamma power responses of all target-selective face electrodes, "hit" and "miss" responses only. Same analysis as in Figure 6, but here trials in which a wrong category was named are not counted among no-recognition trials. Note the similarity to Figure 6.

Quantitative data: Electrode responses

Figure 4 : Individual electrodes

All values except duration are taken from the most significant time-point within 300 ms of target onset. The values for the different electrodes are given in their presentation order: R1, L1, R2, L2.

(A) Recognition – no-recognition difference (in units of S.D.): 0.40 ± 0.10, 0.76 ± 0.19, 0.33 ± 0.09, 0.47 ± 0.12; p value (2-sample, 1-tail t test, see Experimental Procedures): $1.99*10^{-4}$, $1.22*10^{-4}$, $6.18*10^{-4}$, $4.14*10^{-4}$; duration of effect ($p < 0.01$): 465 ms, 335 ms, 150 ms, 285 ms.

(C) Recognition – no-recognition difference (in units of S.D.): -1.96 ± 0.37, -1.88 ± 0.36, -1.26 ± 0.21, -1.33 ± 0.27; p value (2-sample, 2-tail t test, see Experimental Procedures): $8.56*10^{-6}$, $4.71*10^{-6}$, $1.27*10^{-7}$, $3.89*10^{-5}$; duration of effect ($p < 0.01$): 200 ms, 110 ms, 50 ms, 260 ms.

Figure 6: Grand average

Quantitative details for the face electrode grand average. All values except duration are taken from the most significant time-point within 300 ms of target onset. Values given are for evoked and gamma BLP response respectively.

Recognition – no-recognition difference (in units of S.D.): -0.52 ± 0.15, 0.18 ± 0.03; p value (paired t test): $3.50*10^{-3}$, $5.43*10^{-5}$; duration of effect ($p < 0.01$): 95 ms, 585 ms.

Supplemental Experimental Procedures

Electrode localization

Computed tomography (CT) scans following electrode implantation were co-registered to the preoperative MRI using iPlan Stereotaxy software (BrainLAB) to determine electrode positions. The 3-dimensional brain image thus mounted with electrodes locations was normalized to Talairach coordinates (Talairach and Tournoux, 1988) and rendered in BrainVoyager software in 2 dimensions as a surface mesh, enabling precise localization of the electrodes both with relation to the subject's anatomical MRI scan and in standard coordinate space. For joint presentation of all subjects' electrodes and to aid comparison to previous fMRI mapping performed in our lab (see below), electrode locations were projected onto a cortical reconstruction of a specific healthy subject, which is routinely used to visualize results in our mapping studies (Figure 1).

The spatial coverage of the recording electrodes varied among the subjects but typically included temporal, parietal, occipital and frontal lobes. Temporal lobe electrodes were clustered around the Superior Temporal Gyrus (STG), including primary auditory areas, and Medial Temporal Gyrus (MTG), encompassing language areas (possibly Wernicke's area). A sizable group of electrodes were placed in the vicinity of high-order visual areas, including the Lateral Occipital cortex (LO), the Fusiform Gyrus (FG) and the Collateral Sulcus (CoS). Occipital lobe electrodes included several in lower visual areas, some of which were located in V1-V4 proper and some close to the foveal representation. Parietal lobe coverage included BA7 (Brodmann area 7), implicated in visuo-motor coordination, BA39, known to contain part of the "intrinsic" or "default" system, and BA40, in which the Supramarginal Gyrus is located. In the Post-central Gyrus, a large number of electrodes were placed in regions implicated in somatosensory body representation. In the frontal lobe, Precentral Gyrus electrodes covered motor cortex, while other regions covered included BA44 and BA45 (Broca, speech production and understanding), BA46, related to memory retrieval, Inferior Frontal Gyrus (IFG) and Middle Frontal Gyrus (MFG) in BA8, which includes the Frontal Eye-Fields (FEF).

Data Preprocessing

In the preprocessing stage, potential 50 Hz electrical interference was removed from the raw electrical signals using a linear-phase notch FIR filter. Each electrode was de-referenced by subtraction of the averaged signal of all the electrodes, thus discarding non-neuronal contributions from the extracranial reference electrode. The raw signal was then z-normalized per channel.

For calculation of band-limited power (BLP) modulations in a given frequency band, the signal was bandpassed in this frequency range using a linear-phase FIR filter, and the BLP modulation extracted by taking the absolute value of the Hilbert transform (Lachaux et al., 2005) and applying temporal smoothing of 50 ms (custom MATLAB code, The Mathworks Inc.). In both the BM and OC experiments, to offset

the roughly $1/f^2$ profile of the power spectrum, resulting in domination of wide-band (30-70 Hz for gamma) BLP modulations by contribution from the bottom end of the band, we calculated a "flattened" form of the BLP by dividing the entire frequency range into 5 Hz sub-ranges, calculating and scaling the BLP individually in each sub-range by its mean value in the baseline period (250 ms and 500 ms before target onset in the OC and BM experiments, respectively), and finally averaging across sub-ranges. Although, in theory, in view of the said spectral power profile, a more accurate flattening procedure would be to use sub-ranges of exponentially growing width (i.e. a wider window for higher frequencies due to the slower drop in power), our constant-width window flattening yielded almost identical gamma BLPs (typical correlations of above 0.98), due to the high frequencies making up the gamma range (30-70 Hz).

Time-frequency decomposition was based on FFT amplitude spectrum in a 160 ms sliding window with average step size of 6.73 ms. For the induced power spectrograms, the decomposition was done per trial and averaged across trials.

Data processing was carried out using MATLAB. For filtering and time-frequency decomposition, we used original and adapted EEGLAB (Delorme and Makeig, 2004) code.

Statistical analysis

Shuffle control. To validate the significance of the difference in response between the two recognition states in the grand average of all target-selective face electrodes (Figure 6), we used a shuffling control. In each iteration ($N=10^5$) of this control, random behavioral responses were assigned to the BM trials, while keeping the same number of recognition (no-recognition) trials as before. Electrode means were then compared for the two states across electrodes in a paired *t* test, as with the real data. For each time point, the proportion of shuffle iterations in which a more extreme result (*t* statistic) than the real one occurred was taken as the shuffle control *p* value. The results closely replicated the results obtained in the normal paired *t* test (see Figure S14).

Supplemental References

Delorme, A., and Makeig, S. (2004). EEGLAB: an open source toolbox for analysis of single-trial EEG dynamics including independent component analysis. J Neurosci Methods *134*, 9-21.

Lachaux, J.P., George, N., Tallon-Baudry, C., Martinerie, J., Hugueville, L., Minotti, L., Kahane, P., and Renault, B. (2005). The many faces of the gamma band response to complex visual stimuli. Neuroimage *25*, 491-501.

Levy, I., Hasson, U., Avidan, G., Hendler, T., and Malach, R. (2001). Center-periphery organization of human object areas. Nat. Neurosci. *4*, 533-539.

Talairach, J., and Tournoux, P. (1988). Co-Planar Stereotaxic Atlas of the Human Brain (New York: Thieme Medical Publishers).